IV. DISCUSSION OF RESULTS

A. METHOD RESULTS

1. ITTC Single Length Analysis

As previously explained, the ITTC single length analysis, provided in Appendix B, used the Lockheed Froude Numbers to set the model length. Figure 4.1 shows the test tank model drag divided into frictional and residual components. The frictional portion, steadily increases with velocity and the residual resistance is just the difference between the total and frictional resistances. The frictional resistance was Reynolds scaled to predict the ship quantity. Since the ITTC method follows the classical Froude resistance procedure, the residual resistance was not divided into form and wave making components. The entire residual element was Froude scaled to estimate the ship residual component. Figure 4.2 shows the result of combining the ship frictional and ship residual resistances.

For both the model and ship calculations the major component of the total was the residual resistance. This suggested a need to more closely examine the Froude scaled resistances of the SLICE.

The most noticeable characteristic of Figures 4.1 and 4.2 are the two humps. These humps can be related to similar findings with SWATH hulls. Plots of residual resistance coefficients versus Froude Number of SWATH vessels exhibit prismatic humps followed by primary humps (Kennell, 1992). Figure 4.3 shows such a plot for a SWATH

vessel and Figures 4.4 and 4.5 show similar plots for the SLICE model and ship. Whereas the prismatic hump for a SWATH vessel is generally found near a Froude Number of 0.3, the prismatic hump for the SLICE is shifted left to a Froude Number of 0.23. Similarly, the primary hump of a SWATH is found near a Froude Number of 0.5 while the hump appears at 0.31 for the SLICE. These figures show that the residual resistance is the major component of the total in mid-range speeds.

2. ITTC Sectionalized Hull Analysis

The ITTC sectionalized hull analysis is provided in Appendix B. By sectioning the hull, the portion of the test tank model drag associated with friction was increased. Thus, a larger part of the total resistance was dependent on the Reynolds Number and a smaller part was dependent on the Froude Number. Although an equivalent Froude Number based on the equivalent length could be found, the Froude Number used was the same as in the single length calculations. As Figure 4.6 shows, at high speeds the model's frictional percentage was greater than the residual percentage. In the previous analysis, the residual resistance percentage was always greater than the frictional quantity. The result of altering the relative Reynolds and Froude Number dependence in this way was a decrease in predicted ship total resistance, most noticeably at higher speeds.

Although the model's frictional resistance was greater than the residual portion at high speeds, Figure 4.7 shows the same was not true for the ship. This occurs because

when predicting ship quantities, the Froude scaled resistances increase more than the Reynolds scaled ones.

Figures 4.8 and 4.9 show that the prismatic and primary humps are located at the same Froude Numbers as in the previous analysis and there is no sign of an additional hump at higher Froude Numbers. The model friction-residual switch which was shown in Figure 4.6 appears in Figure 4.8 at the corresponding Froude Number. As in Figure 4.7, Figure 4.9 shows that there is not a switch once the quantities have been expanded to the ship. As before, the residual resistance coefficient continues to taper off after the primary hump. And, as in the first case, the residual was the primary source of resistance throughout the speed range of the ship.

3. Hughes Sectionalized Hull Analysis

It was decided to more closely examine the Froude scaled resistances of the SLICE hull. Trying a different approach, the Hughes method was chosen because it further breaks down the residual resistance into form and wave making components. From previous discussion, it was shown that the form drag could be Reynolds scaled and the wave making Froude scaled. The Hughes sectionalizeded hull analysis is provided in Appendix B.

Integral to the Hughes method is the idea that at low Froude Numbers, the wave making resistance is negligible. In fact, this idea was used to find the form factor. Figures 4.10 and 4.11 show the frictional and residual breakdown for this approach. In order to compare this analysis with the ITTC methods, it was necessary to show the

resistance division as a function of the Reynolds and Froude Numbers. Figures 4.12 and 4.13 show the dramatic shift in relative Froude and Reynolds Number dependencies of the Hughes approach. Very apparent is that at high speeds the total drag is almost entirely due to Reynolds dependent resistances whereas for the ITTC cases, the Froude scaled component was dominant.

Figures 4.14 through 4.17 show the plots of resistance coefficients vs. Froude Number for this method. As in the ITTC analyses, once the Froude Number is greater than 0.3, the residual and total coefficients taper off and there is no sign of another hump or increase.

Figures 4.18 and 4.19 show the model division and ship predicted composition of the residual resistance. From the above investigation, an important concept of the procedure was revealed. This method predicts very little wave making resistance at high speeds for the SLICE hull. Note that the Froude scaled resistance equals the wave making resistance. The residual resistance of the sectionalized Hughes analysis is almost entirely from the form drag. A video of the model in the test tank supports the concept of small wave generation at high speeds.

4. Modified Hughes Sectionalized Hull Analysis

Recall that for Froude’s hypothesis and the ITTC scaling procedure, the form drag component was Froude scaled, i.e., constant for each Froude Number. But, in the Hughes analysis, all of the form drag was Reynolds scaled. Since it played such an important role in the Hughes method, a further subdivision of the form drag was undertaken such

that the pod portion was Reynolds scaled and the strut portion was Froude scaled. The modified Hughes sectionalized hull analysis is provided in Appendix B.

Figures 4.20 through 4.23 show the frictional and residual breakdown for the hybrid procedure. In order to compare this analysis with the ITTC methods, the resistance was divided into parts which were functions of the Reynolds and Froude Numbers. Figures 4.24 through 4.27 show that this alteration only slightly shifts the relative Reynolds and Froude Number dependencies back toward the ITTC ratios. Figures 4.28 and 4.29 can be compared to Figures 4.18 and 4.19 of the Hughes method for the purpose of showing the results of varying the residual resistance dependency.

Because of the shift toward Froude scaling, the predicted ship total resistance for this method was slightly higher than the sectionalized Hughes method. It was still considerably lower than both the ITTC analyses.

B. COMPARISON OF METHOD RESULTS

1. Frictional Resistance Comparison

Figure 4.30 compares the model frictional resistance components of the various methods. The single length method’s percentage of the model total resistance was less than the sectioned hull methods. The Hughes and modified Hughes methods used the same frictional resistance values. Figure 4.30 also includes the Lockheed skin friction which was greater than classical ITTC and Hughes assessments. By definition, the Hughes equation yields lower frictional resistance coefficients than the ITTC equation and the two

sectioned hull resistance curves of Figure 4.30 show that. Figure 4.31 shows the ship frictional resistances and the Lockheed ship skin friction. Because they were all Reynolds scaled, the ship frictional resistance curves follow the same trend as the model curves.

2. Residual Resistance Comparison

Figure 4.32 compares the model residual resistances for the various procedures. Also plotted was the Lockheed residual which taken as equal to the Lockheed sum minus the Lockheed skin friction. The single length method gave a larger percentage of the total to the residual resistance compared to the sectioned hull approaches. Note that the Hughes and modified Hughes methods have the same model residual resistances.

Figure 4.33 shows the predicted ship residual resistances for the procedures. The residual resistance was Froude scaled in the ITTC methods but was Reynolds scaled in the Hughes method. The modified Hughes method combined both Reynolds and Froude scaling to predict the ship residual resistance. The figure shows that Froude scaling resulted in higher predicted ship quantities when compared to equivalent Reynolds scaling. Since the modified Hughes method was a combination of the two scaling procedures, the predicted values fell in between the ITTC and Hughes estimates.

Figure 4.34 compares the division of the model residual resistance for the Hughes and modified Hughes methods. Both methods started with the same model total residual resistance and had the essentially the same wave making and

form drag components. Because the form factors were only taken to two decimal points, slight differences on the order of less than a pound do exist between the two method's component values. Since the model figure is only a synopsis of the data, Figure 4.34 only shows one curve for each of these resistance constituents. The modified Hughes method division of strut and pod form drags were also plotted.

Figure 4.35 shows the division of the predicted ship residual resistances for the Hughes and modified Hughes methods. The figure shows that the modified Hughes method predicted higher overall ship residual resistances. The ship wave making resistances for both methods was the same since it was Froude scaled in both instances. Although not explicitly calculated, the predicted ship pod drag of the Hughes method matched the modified Hughes value since it was Reynolds scaled in both methods. Therefore, the source of the increased predicted ship residual resistance was the strut form drag. It was identified that Froude scaling resulted in higher predicted ship values when compared to Reynolds scaling. Since the strut form drag was Froude scaled in the modified Hughes Method, its value was greater than the Hughes method Reynolds scaled counterpart.

From this investigation, one can see that for the modified Hughes method, any variation of the wetted surface area division would result in a ship residual resistance somewhere between the higher ITTC sectioned hull estimate and the lower Hughes sectioned hull estimate. In other words, if the residual resistance has any combination of Reynolds and Froude scaling, the resulting quantity will lie in between the Froude scaled ITTC method and the Reynolds scaled Hughes method.

3. Reynolds Scaled Resistances

Figure 4.36 compares the Reynolds scaled portion of the model resistance for each method and also includes the Lockheed skin friction for the model. The Reynolds resistance equaled the frictional resistance for both the ITTC methods. The Reynolds resistance of the Hughes method included both the frictional and form drag components. The Reynolds scaled resistance of the modified Hughes method was comprised of the frictional resistance and the pod portion of the form drag since the strut drag was Froude scaled.

Figure 4.37 shows the result of Reynolds scaling the model resistances of Figure 4.36. The relative order of the ship curves remained the same. In the residual resistance discussion it was shown that Reynolds scaling predicts lower ship quantities when compared to Froude scaling. It will be shown that the methods which Reynolds scaled larger percentages of the model's total resistance predicted lower ship total resistances.

4. Froude Scaled Resistances

Figure 4.38 compares the Froude scaled portion of the model resistance for each method. The figure also includes the Lockheed residual which was taken as the Lockheed sum minus the Lockheed skin friction. The Froude resistance equaled the residual resistance for both the ITTC methods. The Froude resistance of the Hughes method was the wave making component only and the Froude scaled resistance of

the modified Hughes method included both the wave making and strut portion of the form drag.

Figure 4.39 shows the result of Froude scaling the model resistances of Figure 4.38. The relative order remained the same. It will be shown that assigning larger percentages of the model's total resistance to Froude scaling results in higher ship total resistances since Froude scaling predicts higher ship quantities compared to Reynolds scaling.

The Lockheed residuals were provided in Figures 4.38 and 4.39 for comparative purposes only. It was not within the scope of this thesis to evaluate Lockheed's analysis. It is sufficient to note that the Lockheed evaluation of residual resistance varied from this thesis procedure as evidenced by the difference in model and ship curve shapes for the Lockheed residual resistance.

5. Total Resistance Comparison

All methods started with the same model total resistance. Figure 4.40 compares the predicted ship resistances from each method and Table 1 ranks the ship totals, the frictional and residual divisions of the model and ship. The Lockheed sum, also plotted in Figure 4.40, was less than all analyses covered in the thesis.

The Reynolds and Froude scaled resistance comparison provided the best insight into the analyses of the thesis. Previously, it was stated that Froude scaling a resistance resulted in higher ship values compared to Reynolds scaling. Since the ITTC methods Froude scaled all residual resistances, the ITTC methods predicted the highest ship

total resistances. The Hughes method Reynolds scaled all its residual resistance and therefore predicted the lowest total resistance. The modified Hughes method fell between the ITTC and Hughes method because it applied both Reynolds and Froude scaling to portions of its residual resistance. The sectioned hull procedure provided lower ship total resistances compared to the single length procedure. Table 2 summarizes the Reynolds and Froude Number scaling results.

Rank of Quantities (highest=1, lowest=5)	Model R_F	Model R_R	Ship R_F	Ship R_R	Ship R_T
ITTC Single Length	5	1	5	1	1
ITTC Sectioned Hull	2	4	2	2	2
Hughes Sectioned Hull	3	2	3	4	4
Modified Hughes	3	2	3	3	3
Lockheed	1	5	1	5	5

Table 1. Comparison of method derived frictional, residual and total resistances.

Rank of Quantities (highest=1, lowest=4)	Model R_{Rn}	Model R_{Fn}	Ship R_{Rn}	Ship R_{Fn}	Ship R_T
ITTC Single Length	4	1	4	1	1
ITTC Sectioned Hull	3	2	3	2	2
Hughes Sectioned Hull	1	4	1	4	4
Modified Hughes	2	3	2	3	3

Table 2. Comparison of Reynolds and Froude scaled resistance components.

C. PROPULSION

The ship horsepower or SHP defines whether the ship will meet the desired speed of thirty knots. There are three engines under consideration for the SLICE. The Lycoming TF 40 is the highest rated at 3994 horsepower for continuous operation. With two engines installed and accounting for losses, the delivery of 6850 total installed horsepower is estimated for sustained operation (Lockheed, 1994).

Figure 4.41 shows the predicted SHP versus ship speed and Figure 4.42 shows a close-up of thirty knots. The following observations can be made concerning the desire to cruise at thirty knots. At thirty knots, only the ITTC single length approach estimates a larger horsepower requirement than what the proposed engines can deliver. All other methods suggest that the planned engineering configuration will propel the ship at speeds of greater than thirty knots for sustained operations.

The effective horsepower, EHP, is a means by which a propulsion plant's efficiency can be labeled. It is found by relating the ship total resistance R_{T_S}, in pounds force, and the ship velocity V_S, in feet per second. The 550 in the denominator converts the value to horsepower.

$$EHP = \frac{R_{T_S} V_S}{550} \tag{128}$$

The SHP is found by dividing the effective horsepower EHP by some propulsive coefficient, PC, here equal to 0.73 (Lockheed, 1994).

$$SHP = \frac{EHP}{PC} \tag{129}$$

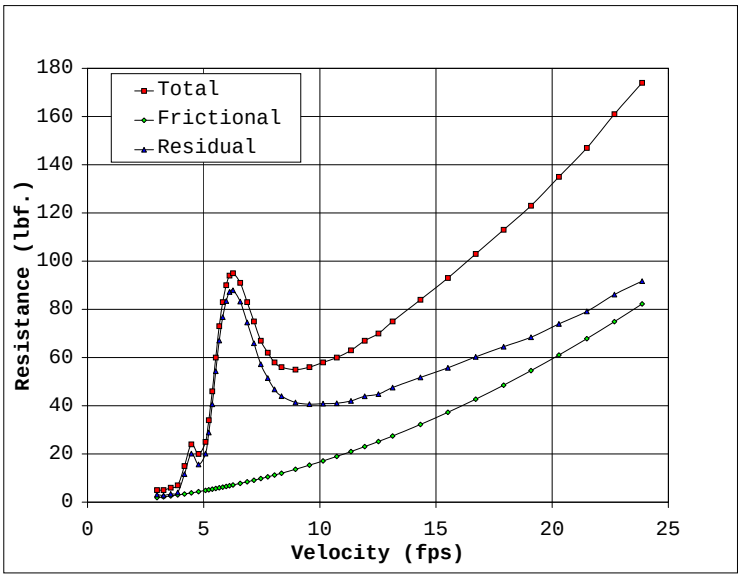

Figure 4.1. ITTC model resistances versus model velocity for a single length analysis of the SLICE hull.

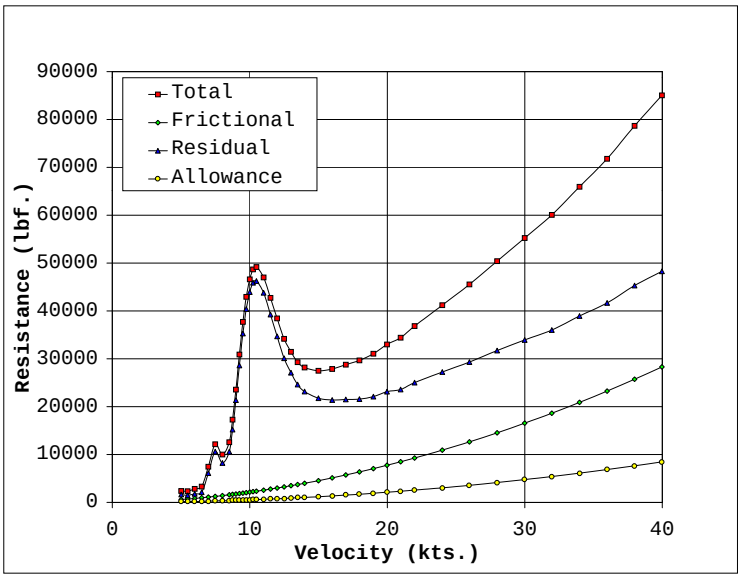

Figure 4.2. ITTC ship resistances versus ship velocity for a single length analysis of the SLICE hull.

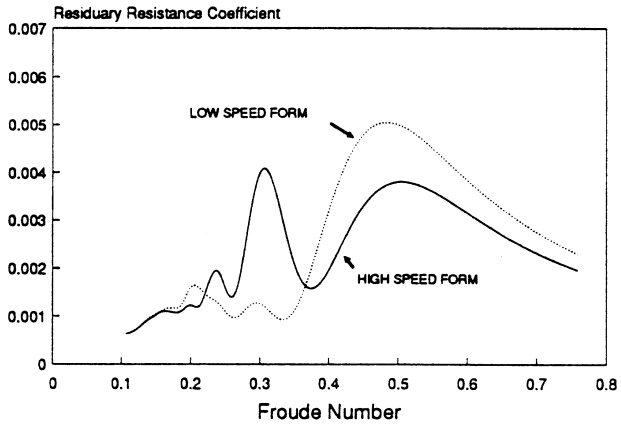

Figure 4.3. Residuary resistance coefficients versus Froude Number (Kennell, 1992).

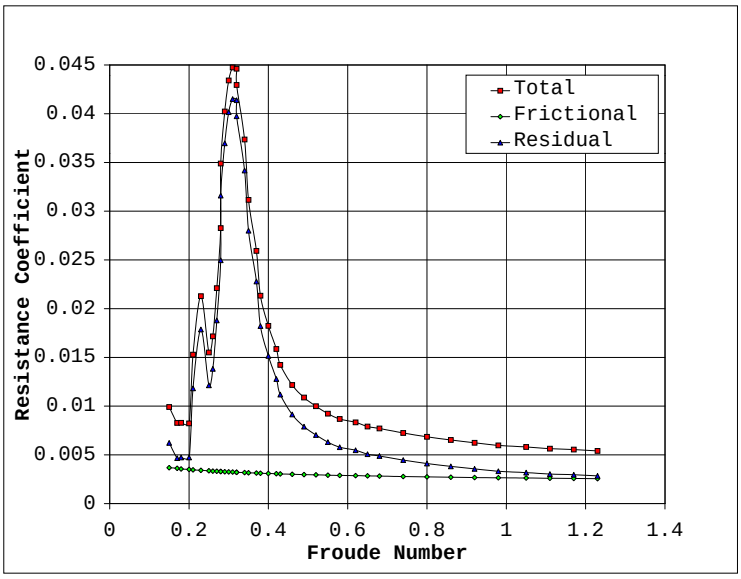

Figure 4.4. ITTC model resistance coefficients versus Froude Number for a single length analysis of the SLICE hull.

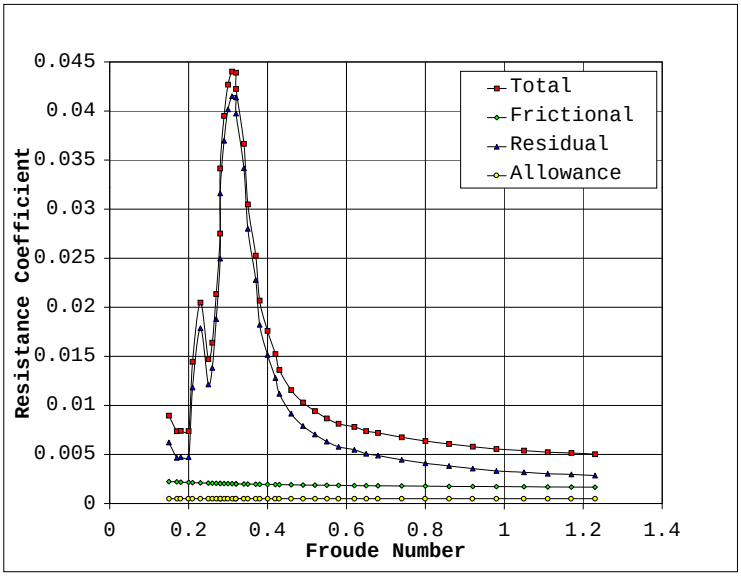

Figure 4.5. ITTC ship resistance coefficients versus Froude Number for a single length analysis of the SLICE hull.

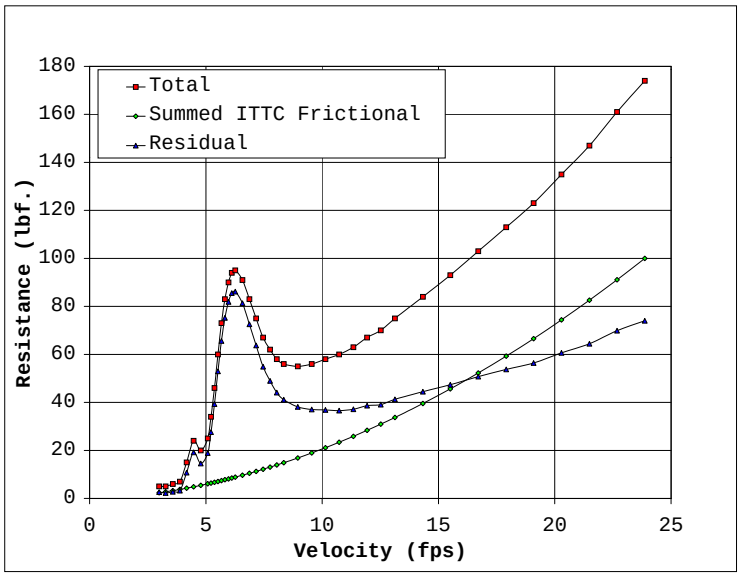

Figure 4.6. ITTC model resistances versus model velocity for the sectionalized SLICE hull.

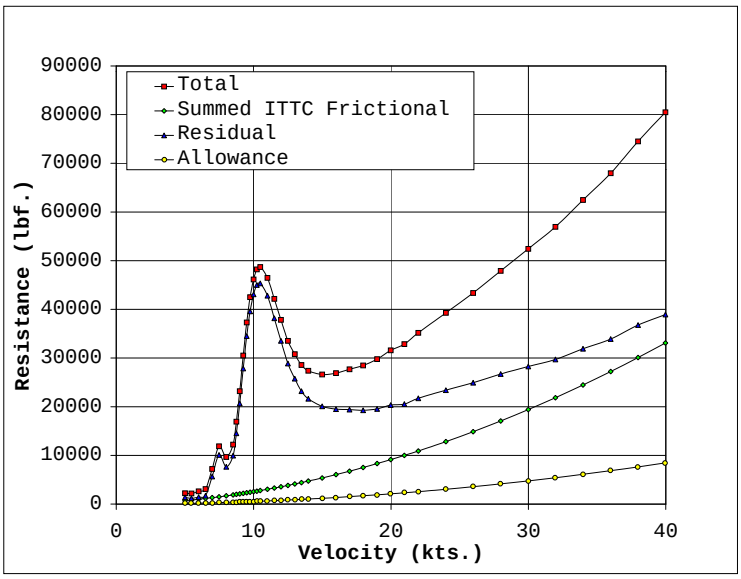

Figure 4.7. ITTC ship resistances versus ship velocity for the sectionalized SLICE hull.

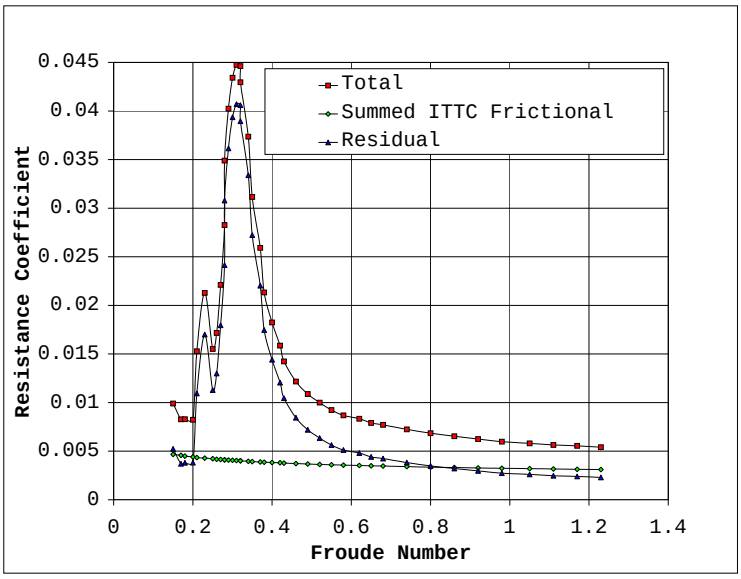

Figure 4.8. ITTC model resistance coefficients versus Froude Number for the sectionalized SLICE hull.

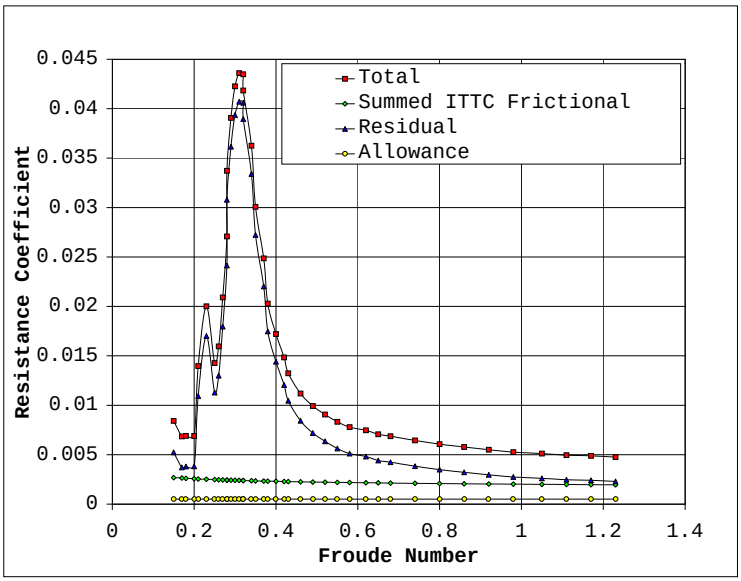

Figure 4.9. ITTC ship resistance coefficients versus Froude Number for the sectionalized SLICE hull.

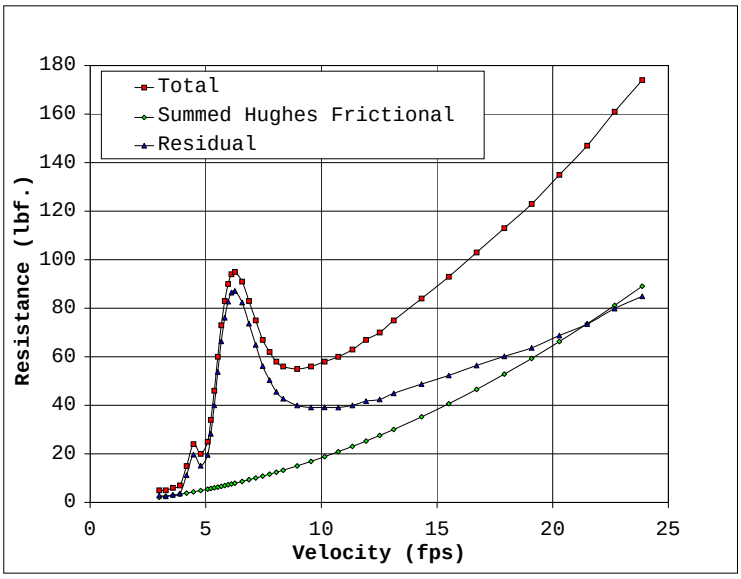

Figure 4.10. Hughes model resistances versus model velocity for the sectionalized SLICE hull.

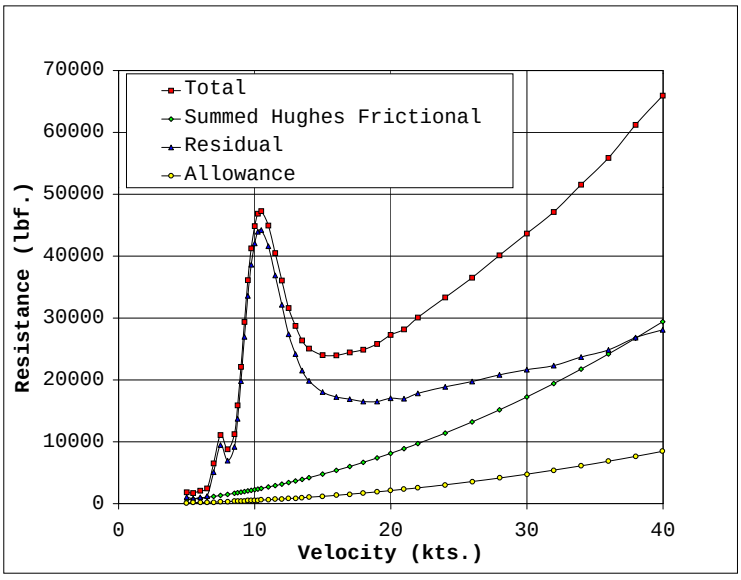

Figure 4.11. Hughes ship resistances versus ship velocity for the sectionalized SLICE hull.

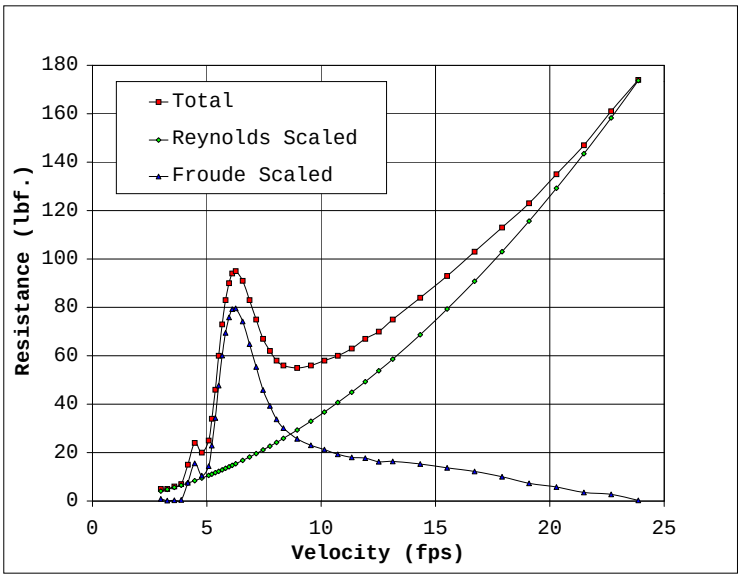

Figure 4.12. Hughes model resistances as functions of Reynolds and Froude Numbers versus model velocity for a sectionalized SLICE hull.

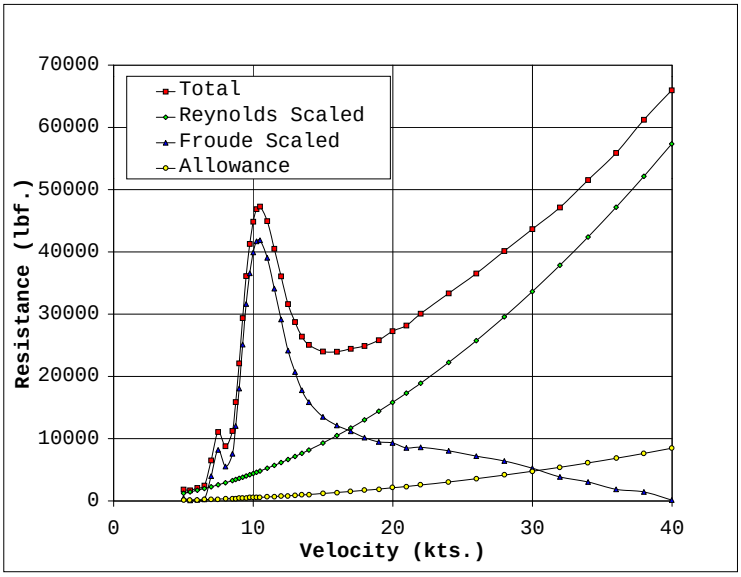

Figure 4.13. Hughes ship resistances as functions of Reynolds and Froude Numbers versus ship velocity for the sectionalized SLICE hull.

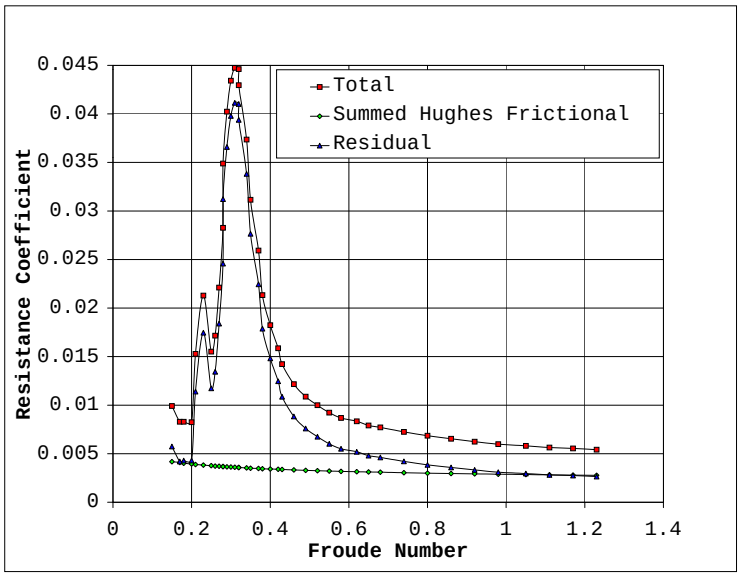

Figure 4.14. Hughes model resistance coefficients versus Froude Number for the sectionalized SLICE hull.

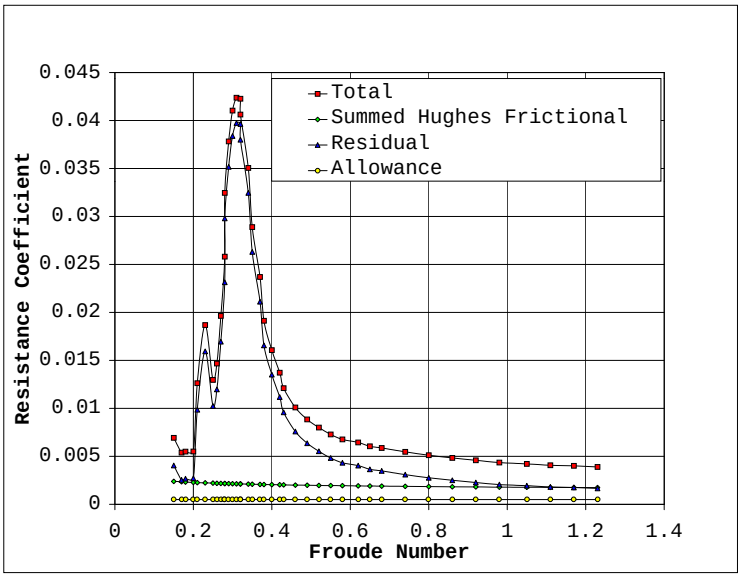

Figure 4.15. Hughes ship resistance coefficients versus Froude Number for the sectionalized SLICE hull.

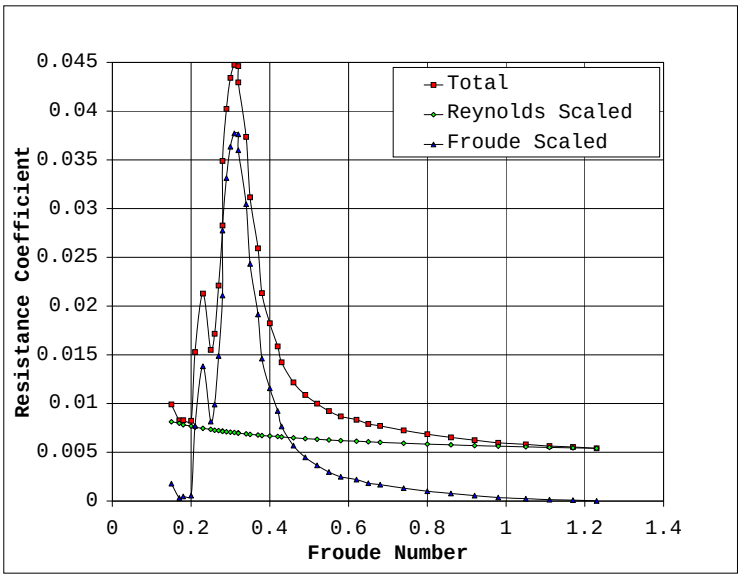

Figure 4.16. Hughes model resistance coefficients as functions of Reynolds and Froude Numbers versus Froude Number for the sectionalized SLICE hull.

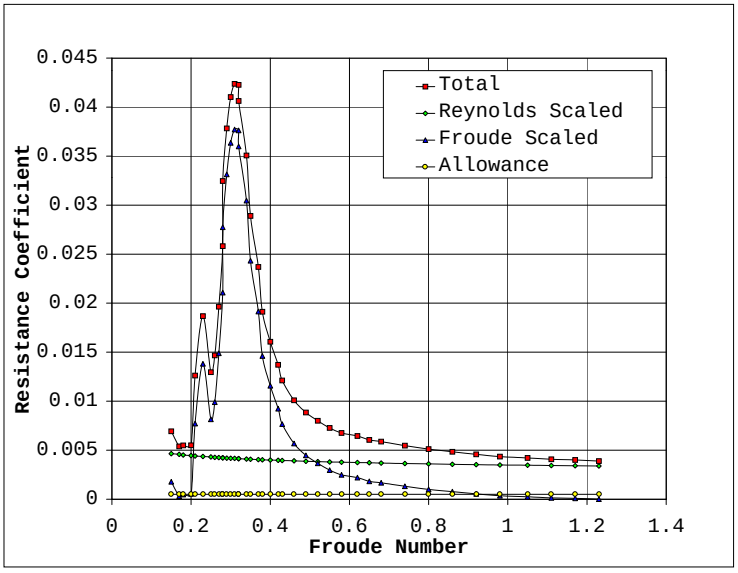

Figure 4.17. Hughes ship resistance coefficients as functions of Reynolds and Froude Numbers versus Froude Number for the sectionalized SLICE hull.

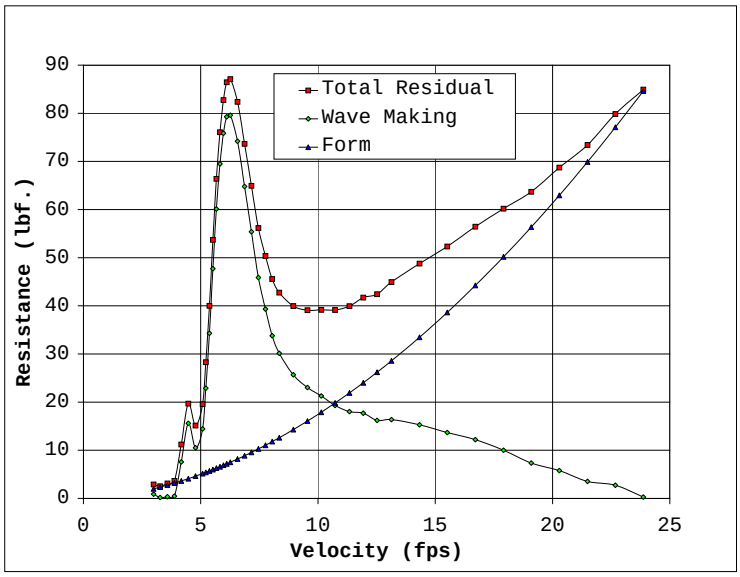

Figure 4.18. Hughes model residual resistances versus model velocity for the sectionalized SLICE hull.

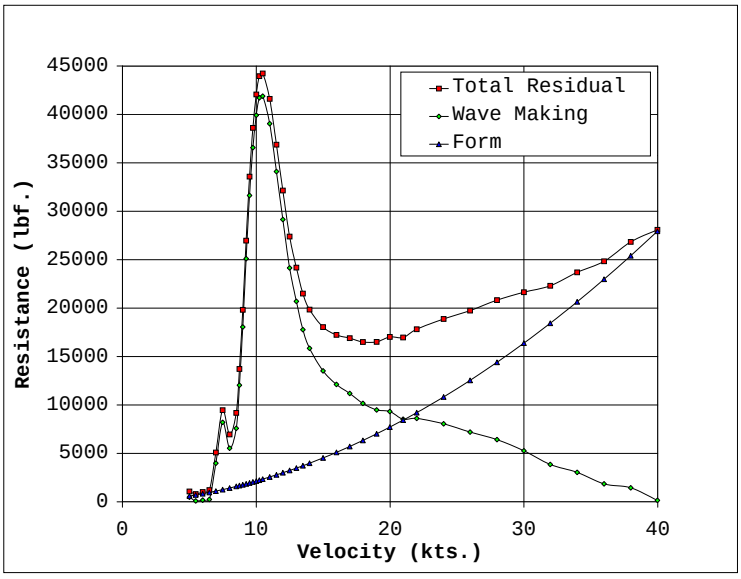

Figure 4.19. Hughes ship residual resistances versus ship velocity for the sectionalized SLICE hull.

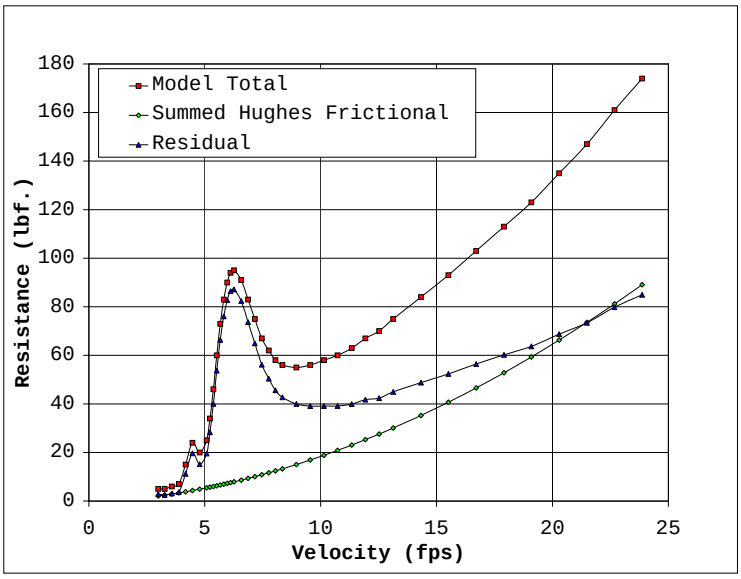

Figure 4.20. Modified Hughes model resistances versus model velocity for the sectionalized SLICE hull.

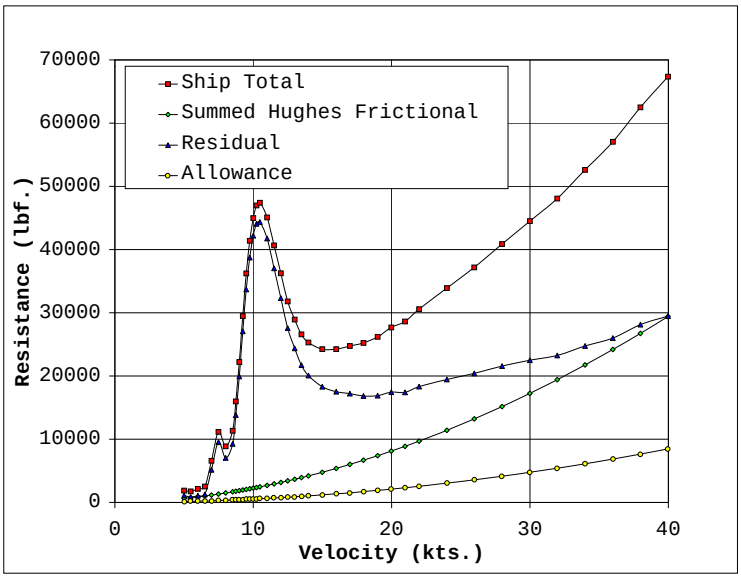

Figure 4.21. Modified Hughes ship resistances versus ship velocity for the sectionalized SLICE hull.

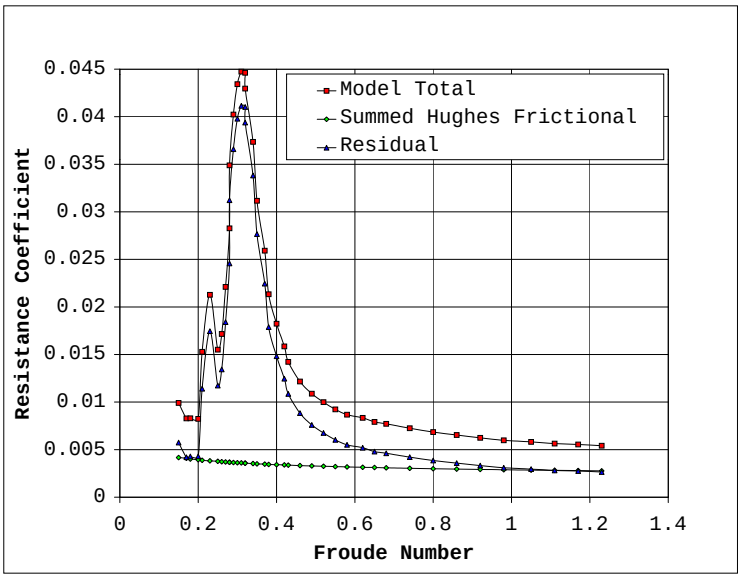

Figure 4.22. Modified Hughes model resistance coefficients versus Froude Number for the sectionalized SLICE hull.

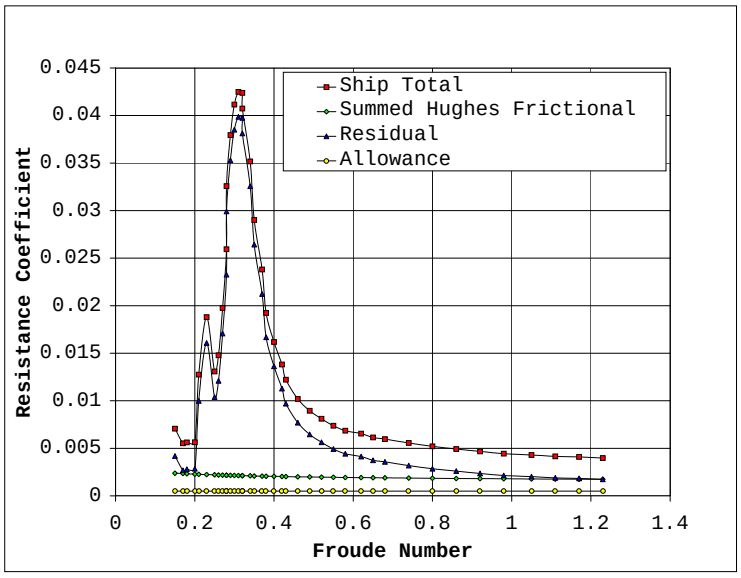

Figure 4.23. Modified Hughes ship resistance coefficients versus Froude Number for the sectionalized SLICE hull.

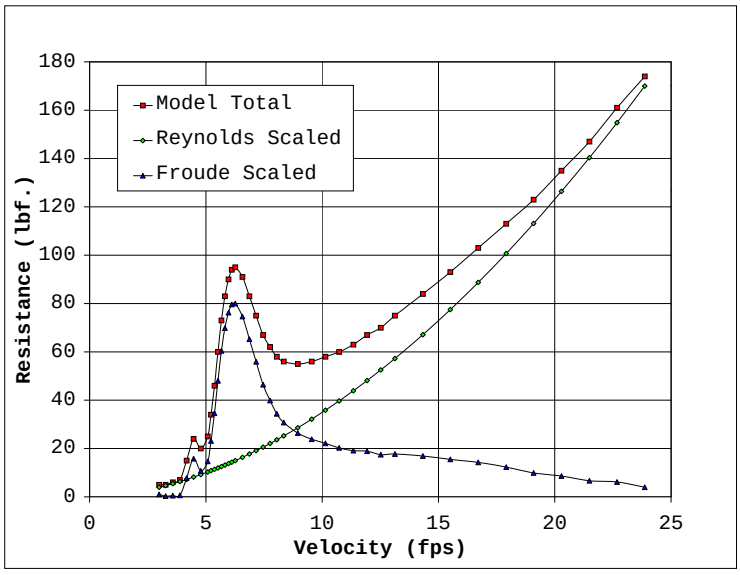

Figure 4.24. Modified Hughes model resistances as functions of Reynolds and Froude Numbers versus model velocity for the sectionalized SLICE hull.

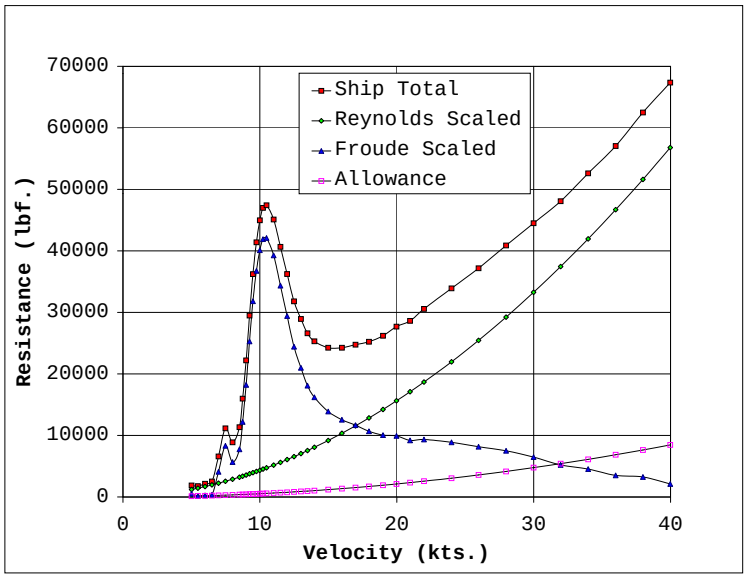

Figure 4.25. Modified Hughes ship resistances as functions of Reynolds and Froude Numbers versus ship velocity for the sectionalized SLICE hull.

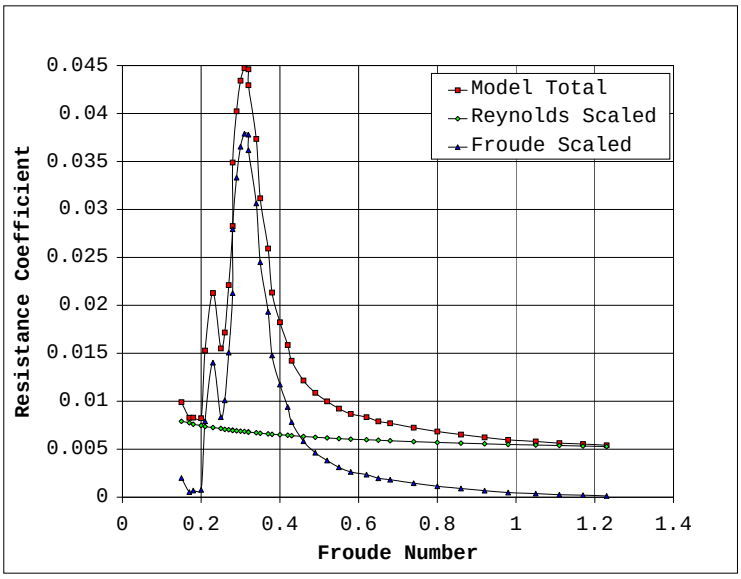

Figure 4.26. Modified Hughes model resistance coefficients as functions of Reynolds and Froude Numbers versus Froude Number for the sectionalized SLICE hull.

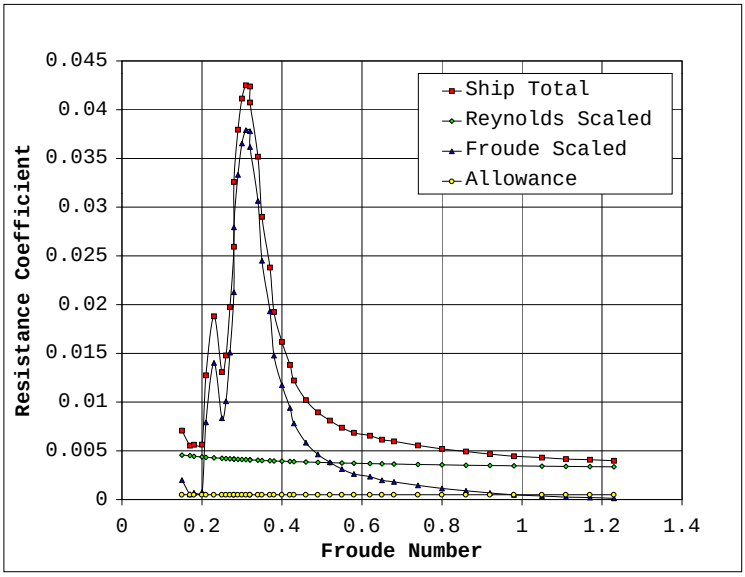

Figure 4.27. Modified Hughes ship resistance coefficients as functions of Reynolds and Froude Numbers versus Froude Number for the sectionalized SLICE hull.

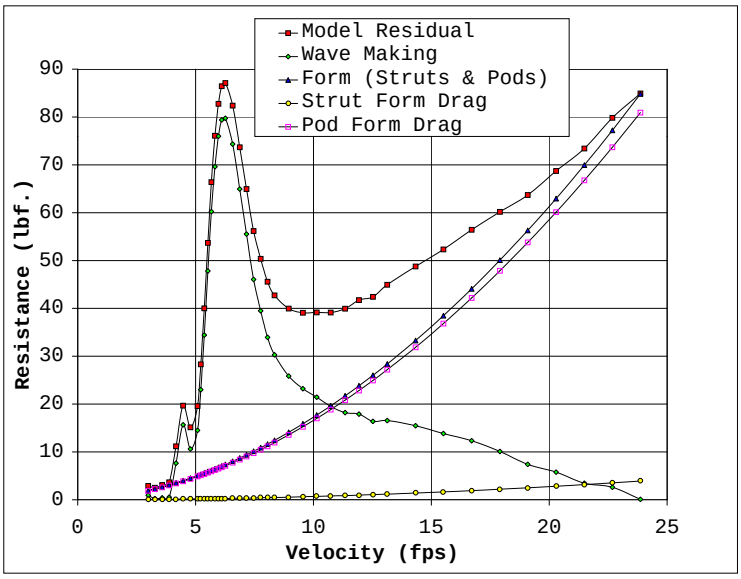

Figure 4.28. Modified Hughes model residual resistances versus model velocity for the sectionalized SLICE hull.

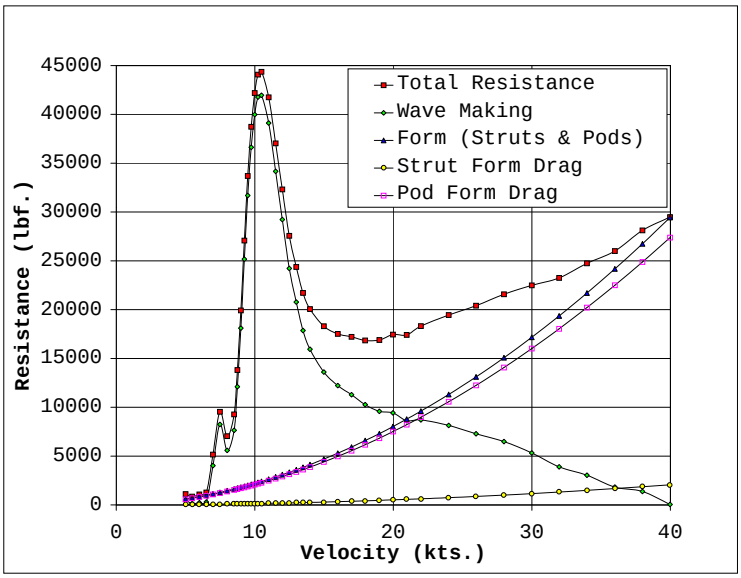

Figure 4.29. Modified Hughes ship residual resistances versus ship velocity for the sectionalized SLICE hull.

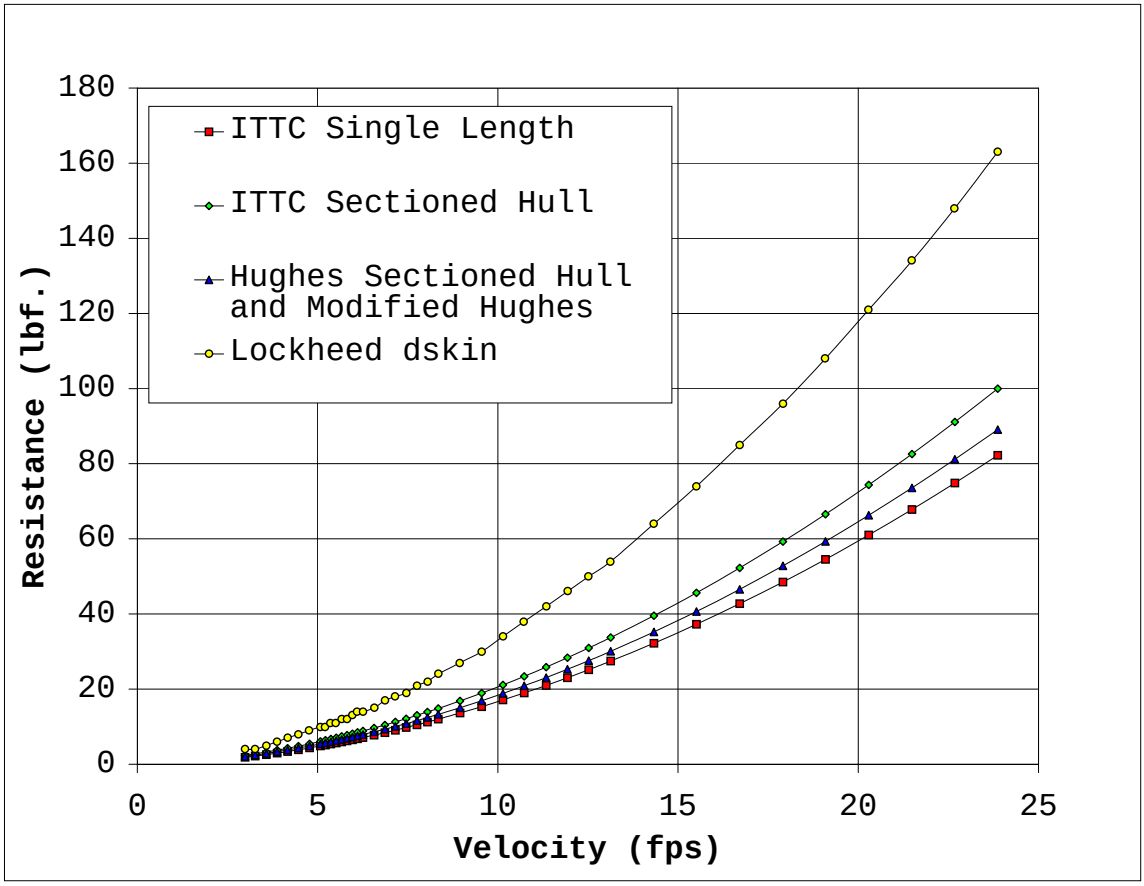

Figure 4.30. Comparison of model frictional resistances.

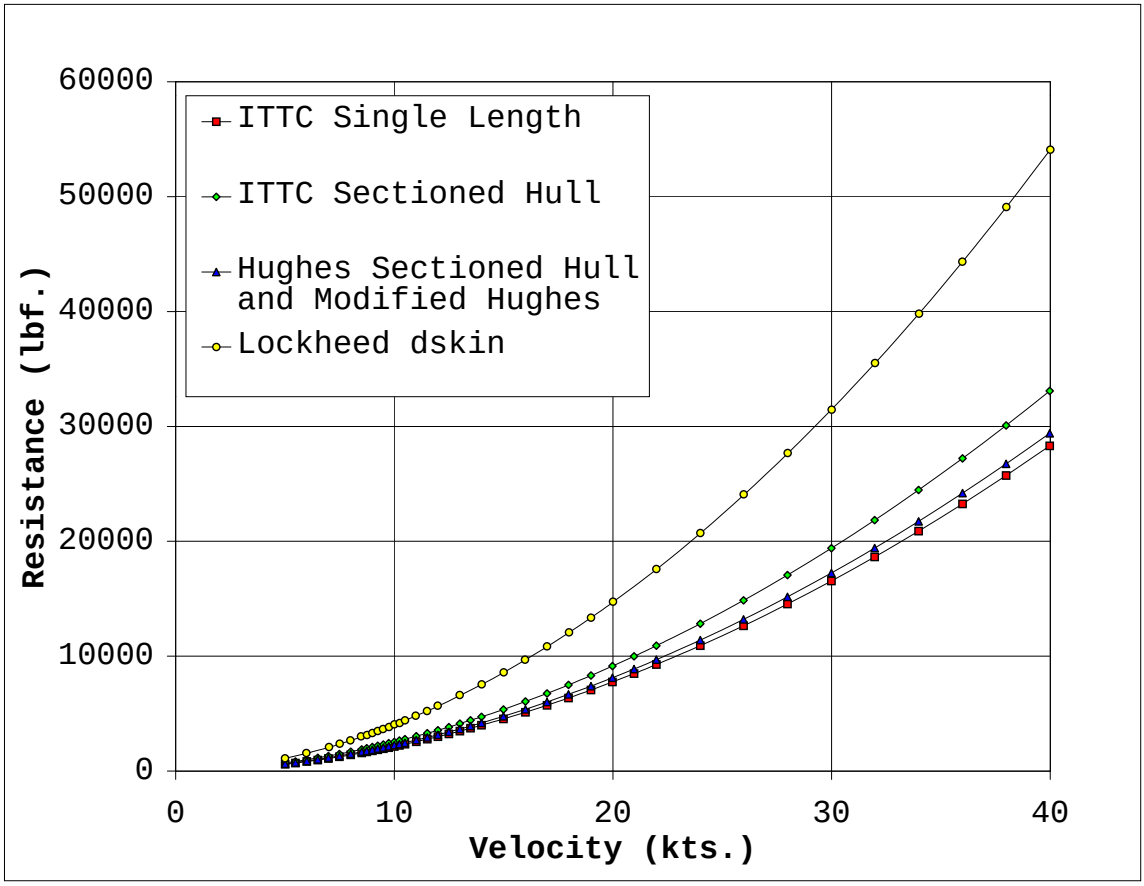

Figure 4.31. Comparison of ship frictional resistances.

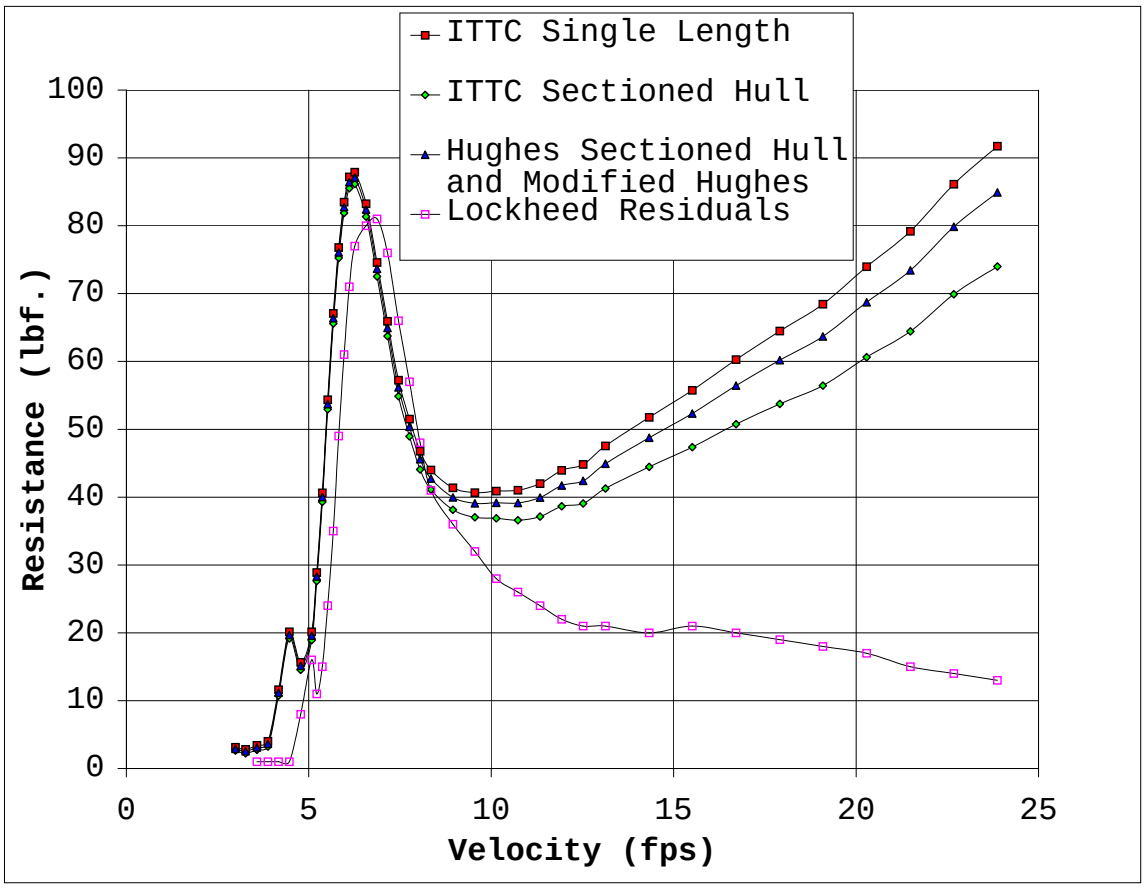

Figure 4.32. Comparison of model residual resistances.

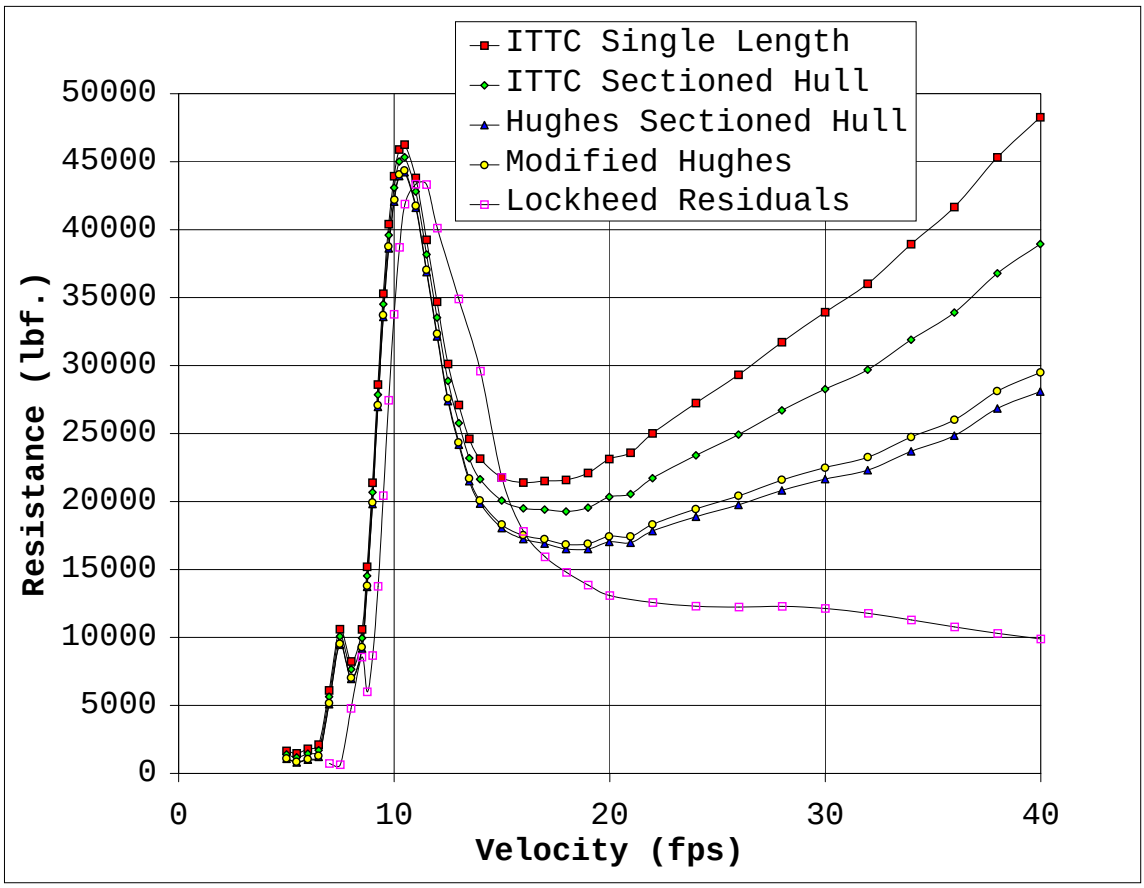

Figure 4.33. Comparison of ship residual resistances.

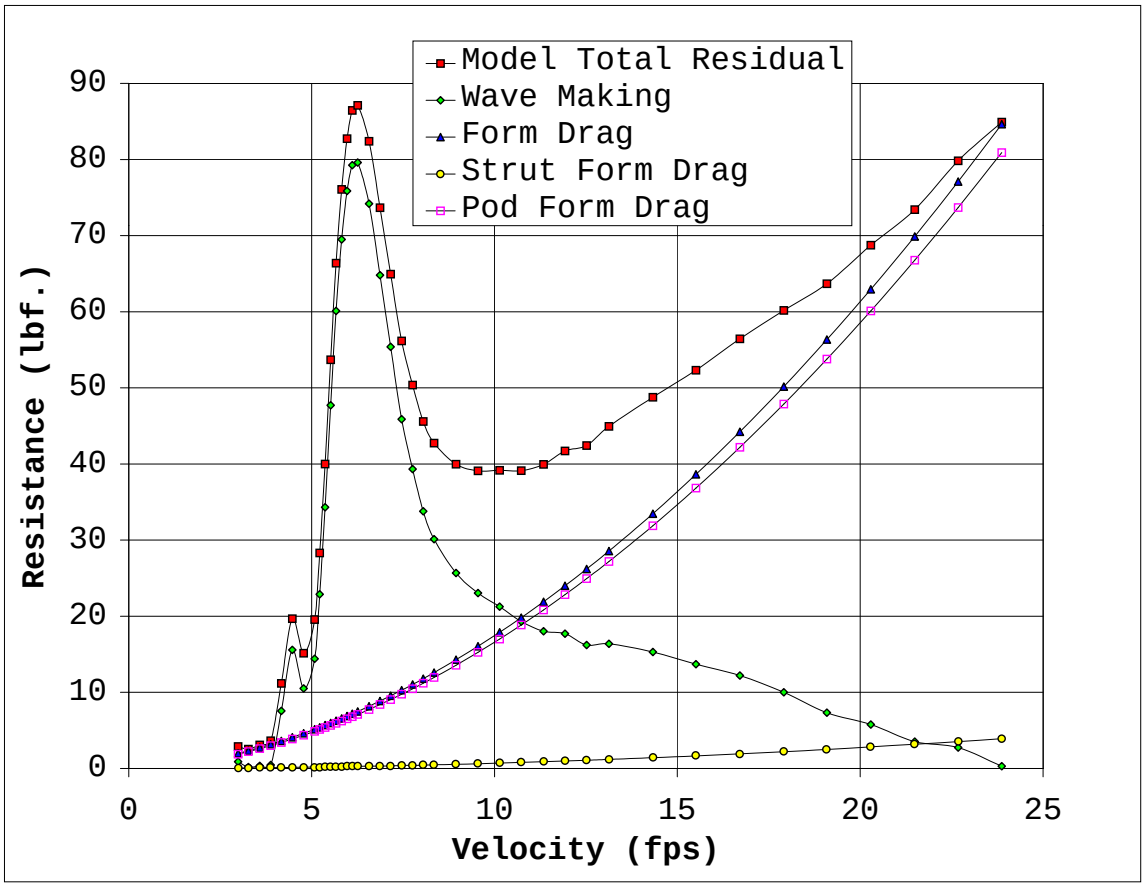

Figure 4.34. Comparison of the model residual resistance division for the Hughes and modified Hughes methods.

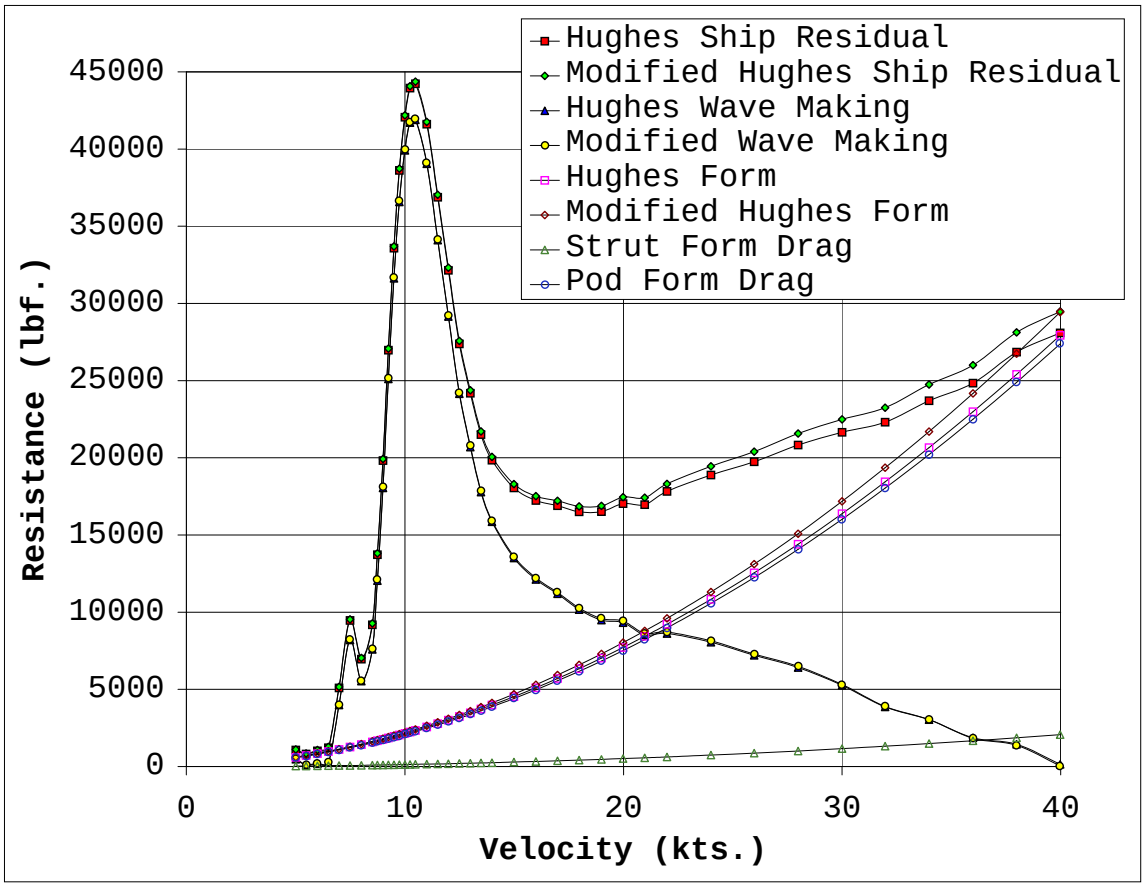

Figure 4.35. Comparison of ship residual resistance division for the Hughes and modified Hughes methods.

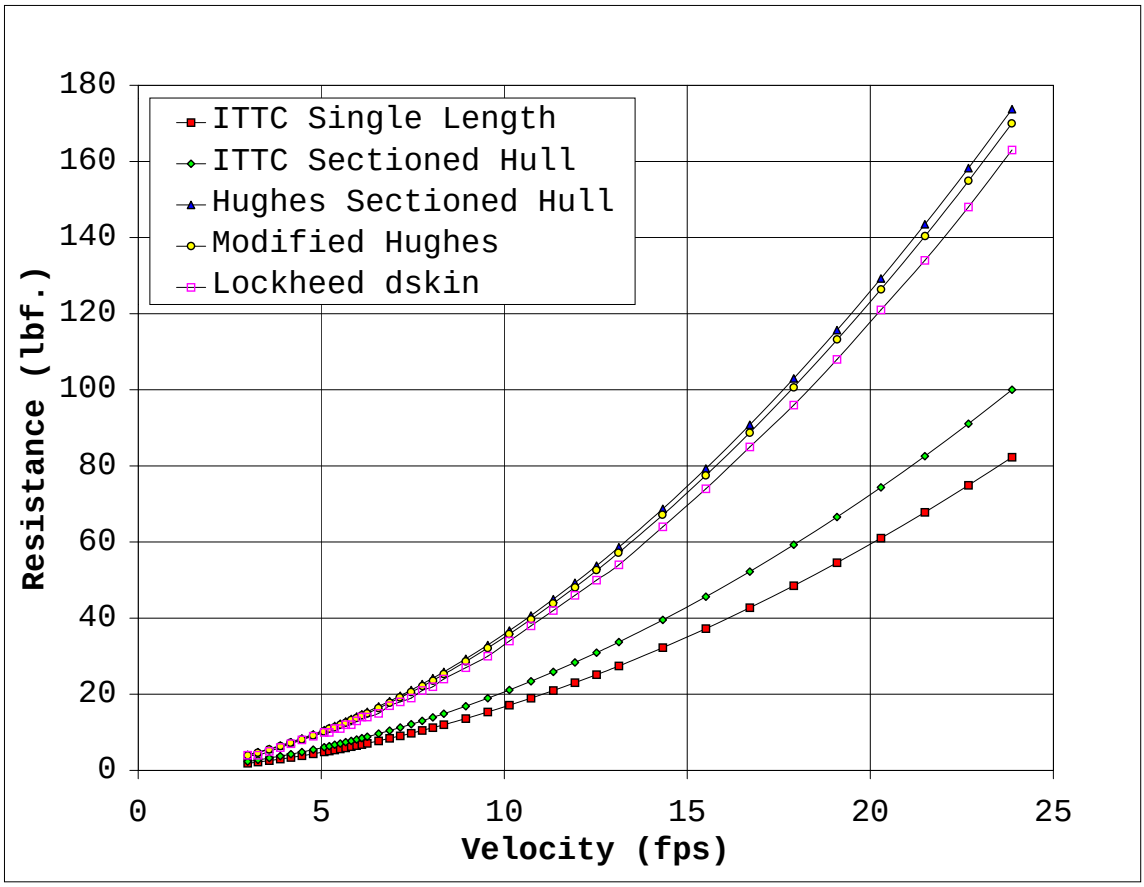

Figure 4.36. Comparison of the Reynolds scaled portion of the model resistance.

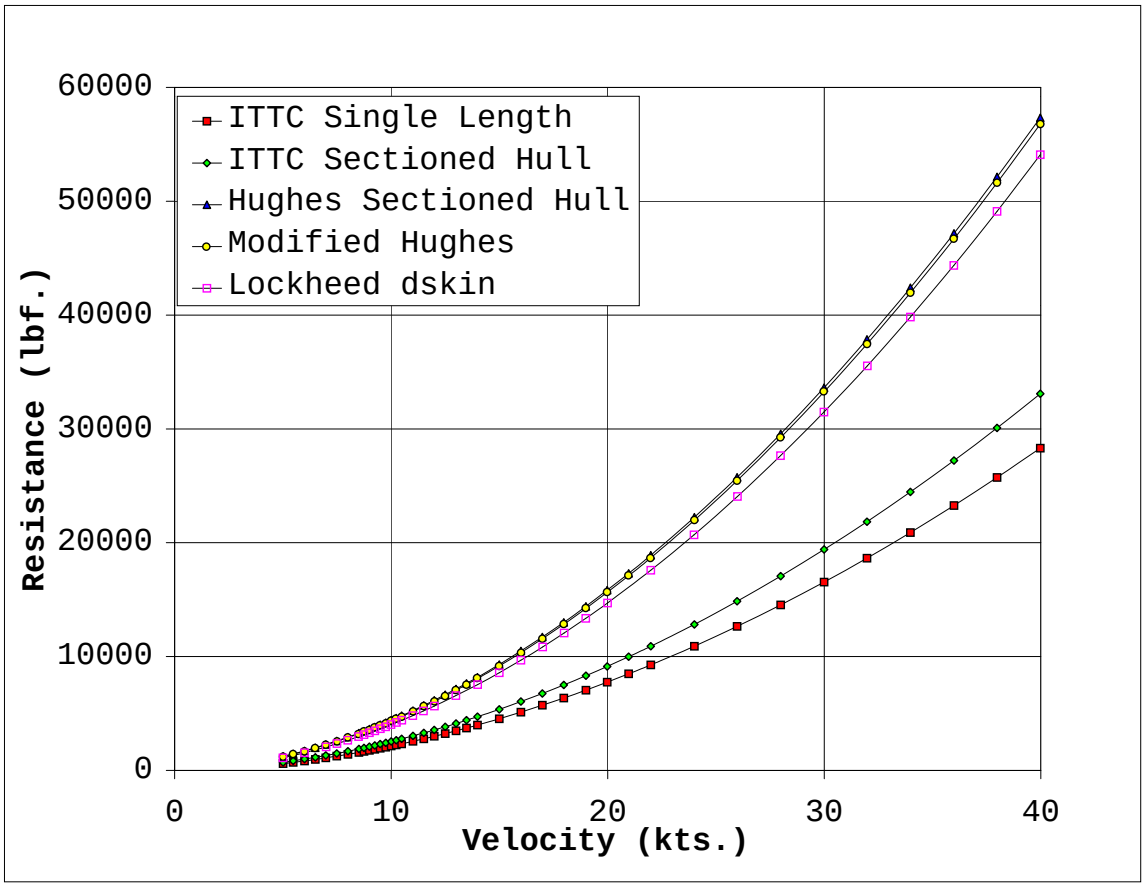

Figure 4.37. Comparison of the ship Reynolds scaled resistances.

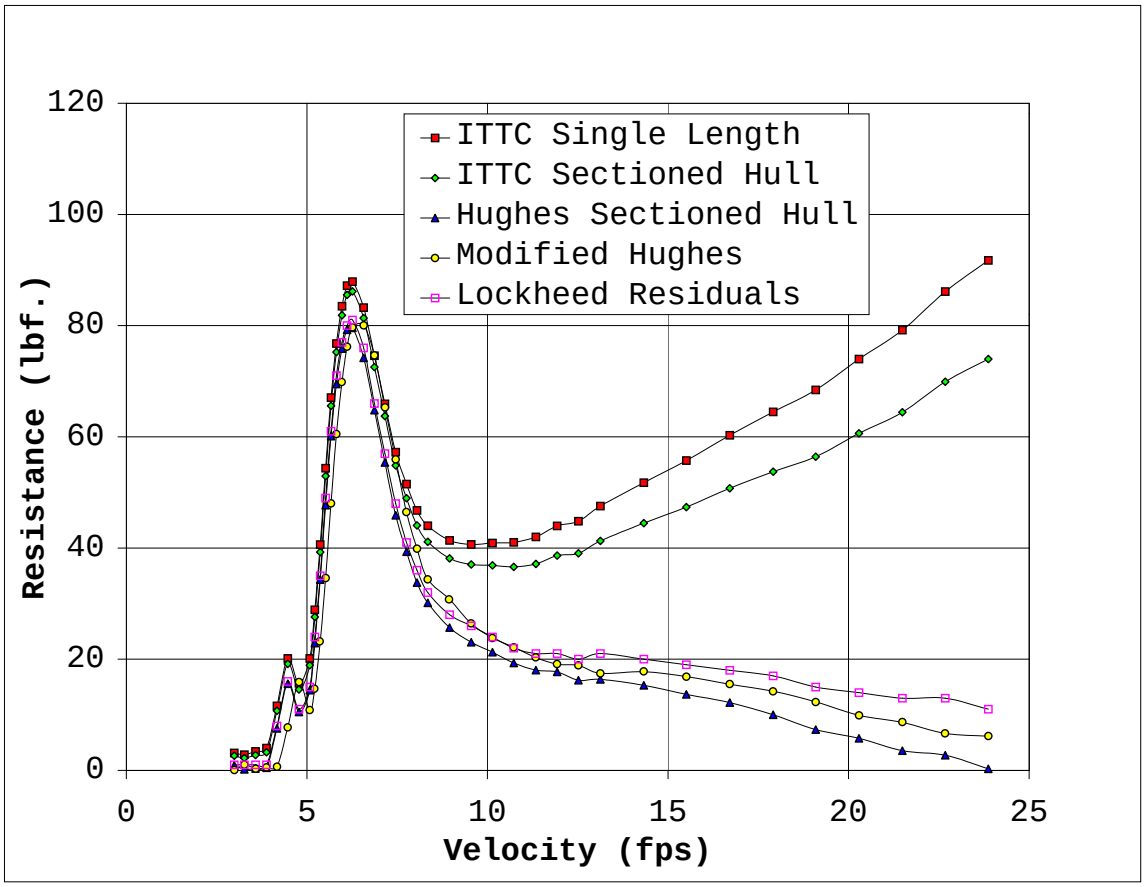

Figure 4.38. Comparison of the Froude scaled portion of the model resistance.

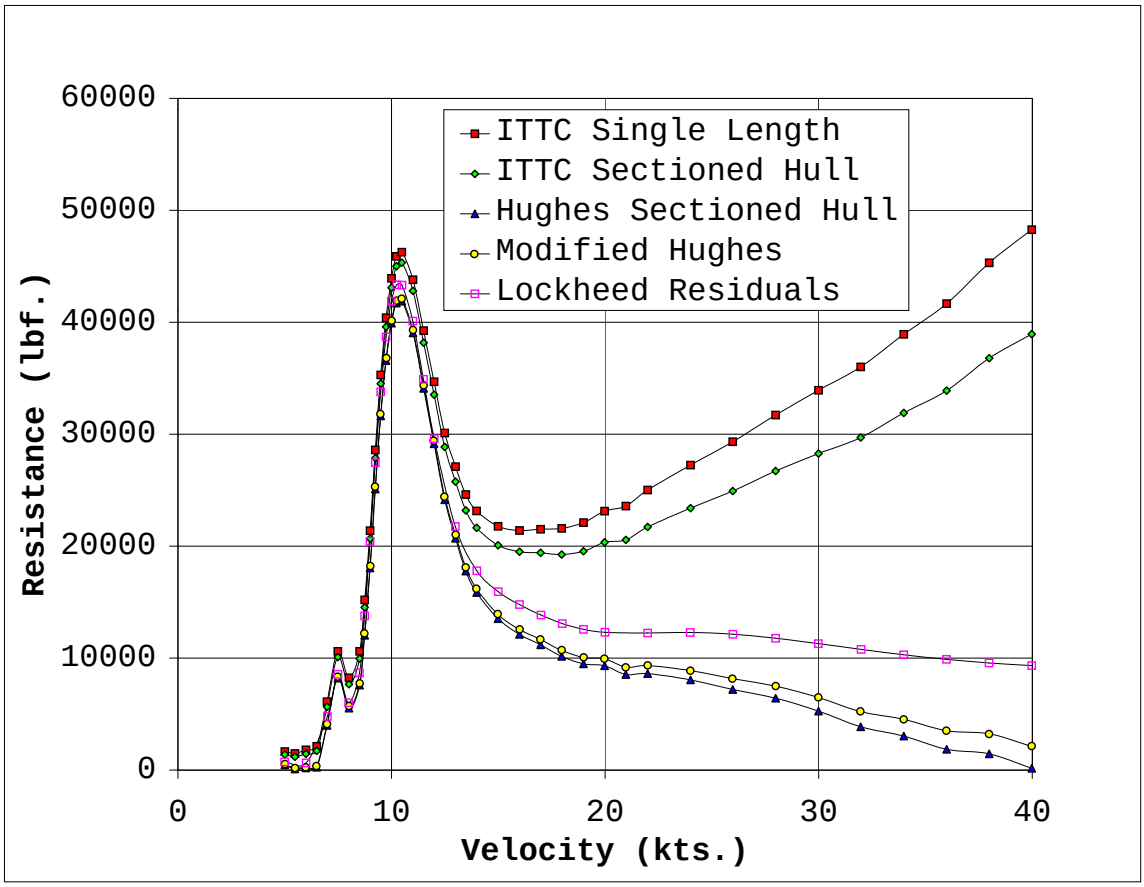

Figure 4.39. Comparison of the ship Froude scaled resistances.

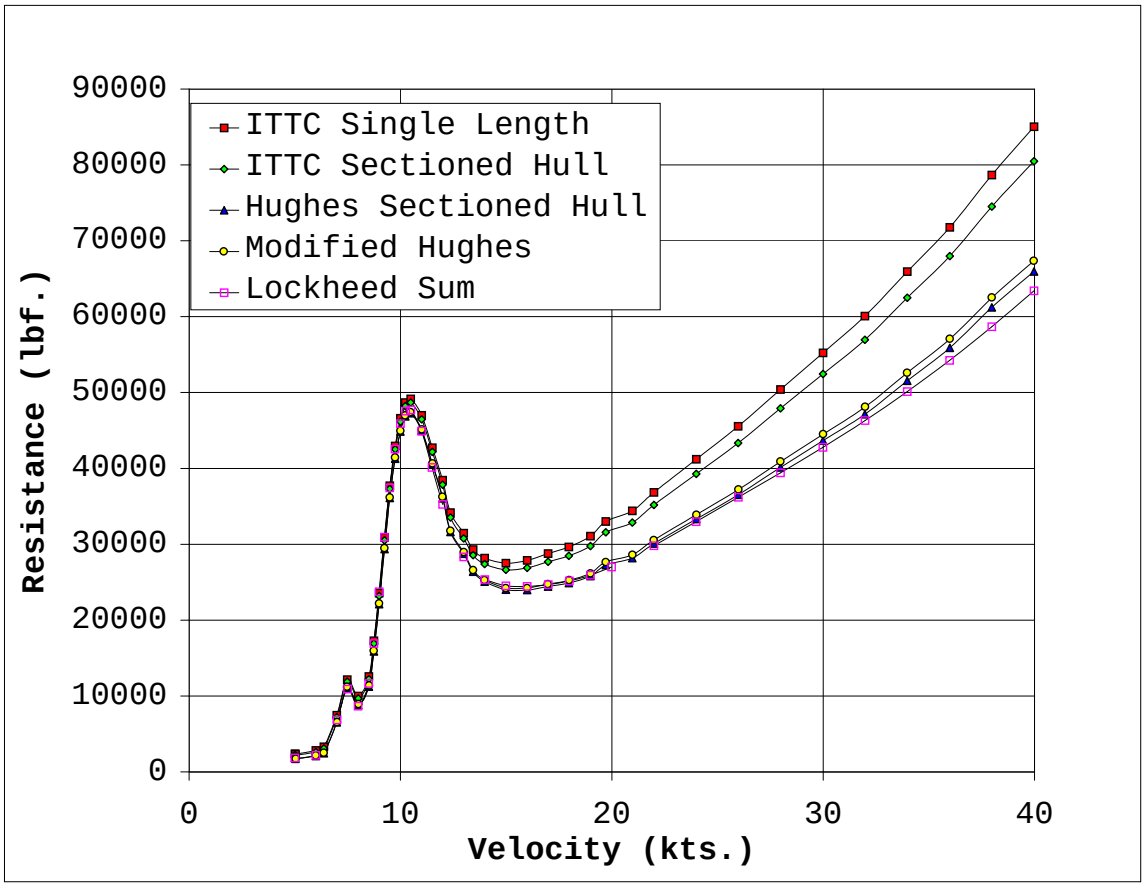

Figure 4.40. Comparison of the ship total resistances.

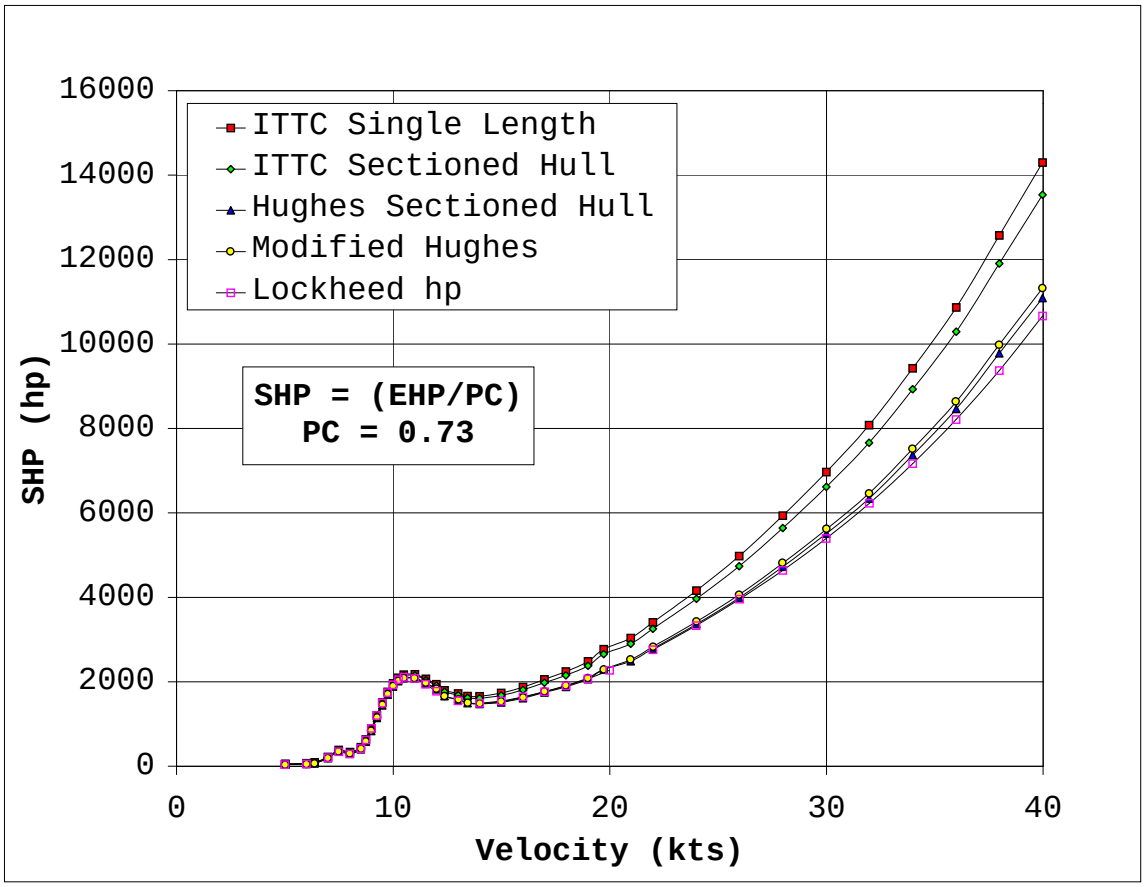

Figure 4.41. Comparison of calculated SHP versus ship velocity.

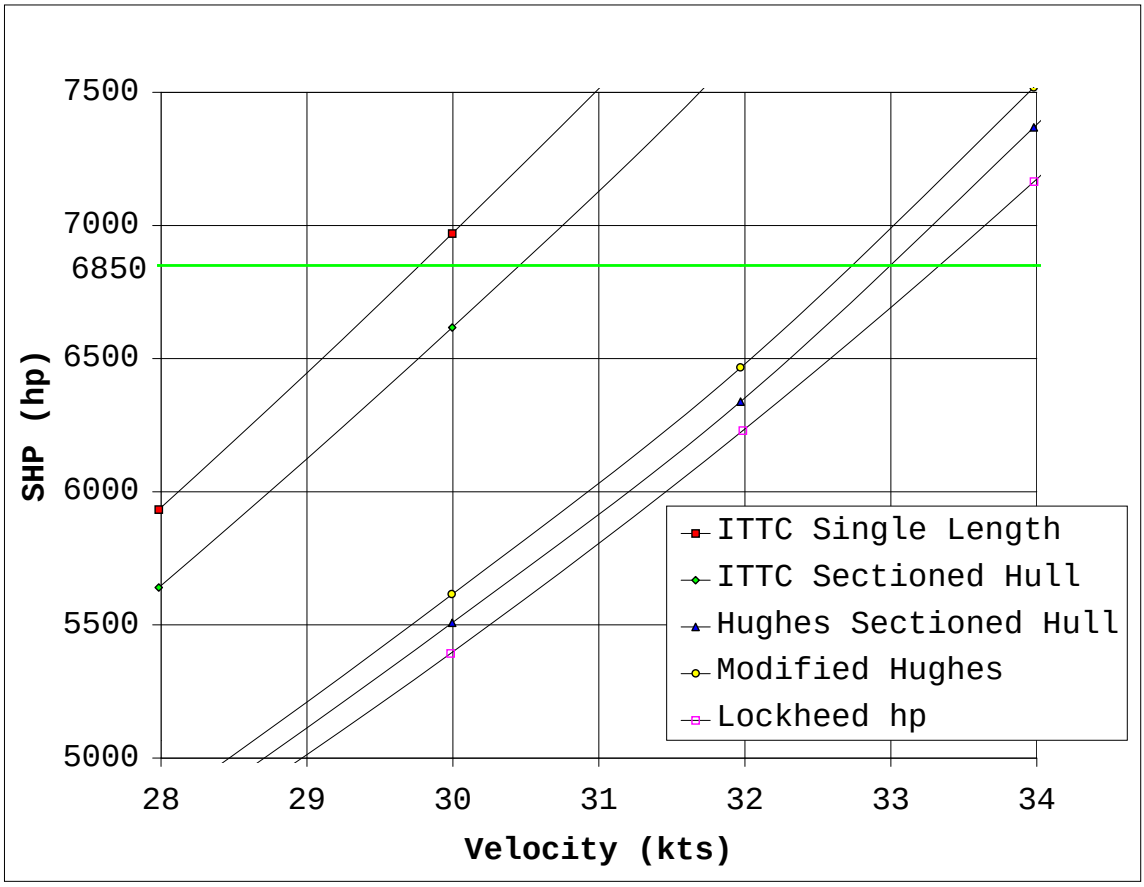

Figure 4.42. Close-up of the SHP curves near 30 knots.